Journal of Solid State Chemistry **168,** 503–508 (2002)
doi:10.1006/jssc.2002.9735

Tetrachloroferrate (III) Salts of BDH-TTP [2,5-Bis(1,3-dithiolan-2-ylidene)-1,3,4,6-tetrathiapentalene] and BDA-TTP [2,5-Bis(1,3-dithian-2-ylidene)-1,3,4,6-tetrathiapentalene]: Crystal Structures and Physical Properties

Koichi Kikuchi,* Hiroyuki Nishikawa,* Isao Ikemoto,* Takashi Toita,† Hiroki Akutsu,† Shin'ichi Nakatsuji,† and Jun-ichi Yamada†,[1]

*Department of Chemistry, Graduate School of Science, Tokyo Metropolitan University, Hachioji, Tokyo 192-0397, Japan; and †Department of Material Science, Graduate School of Science, Himeji Institute of Technology, 3-2-1 Kouto, Kamigori-cho, Ako-gun, Hyogo 678-1297, Japan

Received January 7, 2002; in revised form March 19, 2002; accepted April 3, 2002

Three $FeCl_4$ salts based on non-tetrathiafulvalene (TTF) donors, 2,5-bis(1,3-dithiolan-2-ylidene)-1,3,4,6-tetrathiapentalene (BDH-TTP) and 2,5-bis(1,3-dithian-2-ylidene)-1,3,4,6-tetrathiapentalene (BDA-TTP), have been prepared and characterized as κ-(BDH-TTP)$_2$FeCl$_4$, β-(BDA-TTP)$_2$FeCl$_4$, and (BDA-TTP)$_3$FeCl$_4$ · PhCl. The κ-(BDH-TTP)$_2$FeCl$_4$ salt, with a room-temperature conductivity (σ_{rt}) of 39 S cm^{-1}, is metallic down to 1.5 K, and its magnetic susceptibility obeys the Curie–Weiss law with a Curie constant (C) of 4.25 emu K mol^{-1} and a Weiss constant (θ) of 0.041 K. β-(BDA-TTP)$_2$FeCl$_4$ exhibits metallic behavior (σ_{rt} = 9.4 S cm^{-1}) with a sharp metal-to-insulator (MI) transition (T_{MI} = 113 K) and antiferromagnetic ordering with the Néel temperature of near 8.5 K, whereas the solvated (BDA-TTP)$_3$FeCl$_4$ · PhCl salt is a semiconductor with a thermal activation energy of 0.11 eV ($\sigma_{rt} = 2.0 \times 10^{-2}$ S cm^{-1}) and exhibits Curie–Weiss behavior (C = 4.42 emu K mol^{-1}, $\theta = -0.35$ K). © 2002 Elsevier Science (USA)

Key Words: **non-TTF donor; crystal structure; conductivity; magnetic susceptibility; metallic behavior; antiferromagnetic ordering.**

INTRODUCTION

Recent studies on the development of molecular magnetic conductors by combining organic π-electron donors and inorganic paramagnetic anions have resulted in a new class of charge-transfer (CT) salts, such as an antiferromagnetic organic metal (1), ferromagnetic organic metals (2), and antiferromagnetic organic metals exhibiting superconductivity (3), in which magnetic order and metallic conductivity coexist. However, these CT salts are derived from tetrachalcogenafulvalene (TCF) donors. Therefore, the successful formation of this class of multiproperty molecular materials consisting of non-TCF donors and paramagnetic anions has obvious appeal, but it has proven to be a challenge. For example, the $CuBr_2$ complexes based on new bis(1,3-dithiol-2-ylidene) donors containing no tetrathiafulvalene (TTF) unit has been studied, but these complexes failed to exhibit metallic conducting behavior (4). Meanwhile, we have found that (i) 2,5-bis(1,3-dithiolan-2-ylidene)-1,3,4,6-tetrathiapentalene (BDH-TTP, Fig. 1), a sulfur-based non-TTF donor, provides many metallic CT salts stable down to low temperatures regardless of the counteranions used (5) and (ii) new superconducting salts can be obtained from a dithiane analog of BDH-TTP, 2,5-bis(1,3-dithian-2-ylidene)-1,3,4,6-tetrathiapentalene (BDA-TTP, Fig. 1), in combination with relatively large anions such as SbF_6^-, AsF_6^-, and PF_6^- (6). Our attention was thus focused on the Fe-containing BDH-TTP and BDA-TTP salts. In this paper we report the crystal structures and physical properties of κ-(BDH-TTP)$_2$FeCl$_4$, β-(BDA-TTP)$_2$FeCl$_4$, and (BDA-TTP)$_3$FeCl$_4$ · PhCl (7)

EXPERIMENTAL

Synthesis

BDH-TTP and BDA-TTP were synthesized following our reported methods (5, 6), Electrocrystallization of BDH-TTP (0.08 mmol) with Et_4NFeCl_4 (0.43 mmol) in 5% EtOH/PhCl (60 ml) by the controlled-current method (8) gave (BDH-TTP)$_2$FeCl$_4$. On the other hand, electrocrystallization of BDA-TTP under the same conditions

[1] To whom correspondence should be addressed. Fax: + 81(0)791-58-0164. E-mail: yamada@sci.himeji-tech.ac.jp.

0022-4596/02 $35.00

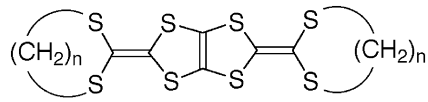

FIG. 1. BDH-TTP and BDA-TTP donors.

furnished two types of crystals, $(BDA\text{-}TTP)_2FeCl_4$ and the solvated $(BDA\text{-}TTP)_3FeCl_4 \cdot PhCl$ salt.

Structure Determination

The data of X-ray structures were collected on a Bruker SMART-APEX three-circle diffractometer equipped with a CCD area detector [for $(BDH\text{-}TTP)_2FeCl_4$ and $(BDA\text{-}TTP)_3FeCl_4 \cdot PhCl$] and on a Rigaku AFC7R diffractometer [for $(BDA\text{-}TTP)_2FeCl_4$]. The structures were solved by direct methods and refined by full-matrix least-squares analysies. The structure of $(BDA\text{-}TTP)_3FeCl_4 \cdot PhCl$ was refined as a racemic twin with the twin parameters refining to 0.69(5). All diagrams and calculations were performed using SHELXTL software. The overlap integrals S_{ij} between HOMOs of adjacent donor molecules were calculated on the basis of the extended Hückel MO method by using the parameters reported in the literature (9).

Physical Measurements

Electrical conductivity was measured by the four-probe dc technique using gold wire contacted to a gold electrode deposited on the surface of a single crystal by thermal evaporation or with gold paste. Susceptibility measurements were made with a Quantum Design MPMS-5 SQUID magnetometer from 300 to 2 K at an external field of 1 kOe. The magnetic field dependence of susceptibilities was measured up to 50 kOe.

RESULTS AND DISCUSSION

Crystal Structures

Crystallographic data for κ-$(BDA\text{-}TTP)_2FeCl_4$, β-$(BDA\text{-}TTP)_2FeCl_4$, and $(BDA\text{-}TTP)_3FeCl_4 \cdot PhCl$ are summarized in Table 1.

TABLE 1
Crystallographic Data of κ-$(BDA\text{-}TTP)_2FeCl_4$, β-$(BDA\text{-}TTP)_2FeCl_4$ and $(BDA\text{-}TTP)_3FeCl_4 \cdot PhCl$

	κ-$(BDA\text{-}TTP)_2FeCl_4$	β-$(BDA\text{-}TTP)_2FeCl_4$	$(BDA\text{-}TTP)_3FeCl_4 \cdot PhCl$
Formula	$C_{20}H_{16}S_{16}FeCl_4$	$C_{24}H_{24}S_{16}FeCl_4$	$C_{42}H_{41}S_{24}FeCl_5$
Formula weight	966.94	1023.04	1548.29
Temperature (K)	293	293 [95]	293
Wavelength (Å)	0.71073 (Mo$K\alpha$)	0.71073 (Mo$K\alpha$)	0.71073 (Mo$K\alpha$)
Crystal system	Orthrhombic	Monoclinic	Monoclinic
Space group	*Pnma*	$P2_1/a$	$P2_1$
a (Å)	11.0388(15)	12.452(7) [12.381(2)]	9.7717(15)
b (Å)	37.471(5)	38.72(1) [38.686(7)]	35.639(6)
c (Å)	8.1693(1)	7.731(4) [7.5899(3)]	8.8584(14)
α (deg)	90	90	90
β (deg)	90	91.17(4) [91.065(3)]	92.085(3)
γ (deg)	90	90	90
V (Å^3)	3379.1(8)	3727(3) [3624.4(11)]	3083.0(8)
Z	4	4	2
D_{calced} (Mg m^{-3})	1.901	1.823 [1.875]	1.668
μ (mm^{-1})	1.770	1.611 [1.656]	1.308
Crystal size (mm)	$0.4 \times 0.2 \times 0.05$	$0.5 \times 0.2 \times 0.05$	$0.5 \times 0.25 \times 0.07$
Crystal color	Black	Black	Pale black
θ range (deg)	2.17–23.26	2.10–27.76	2.81–28.33
Total no. of reactions	14,299	9069 [22,705]	14,121
No. of unique reflections	2490	8692 [8304]	6441
No. of reflections observed	2094 [$I > 2\sigma(I)$]	4289 [$I > 3\sigma(I)$] [7088 [$I > 2\sigma(I)$]]	3828 [$I > 2\sigma(I)$]
No. of parameters	190	409 [406]	620
R_1, wR_2	0.0298, 0.0754	0.0407, 0.1122 [0.0296, 0.0772]	0.0484, 0.1005
GOF	1.035	1.169 [0.990]	0.842
$\Delta\rho_{max}/\Delta\rho_{min}$ (e Å^{-3})	0.389/−0.313	0.118/−0.265 [0.532/−0.306]	0.073/−0.329

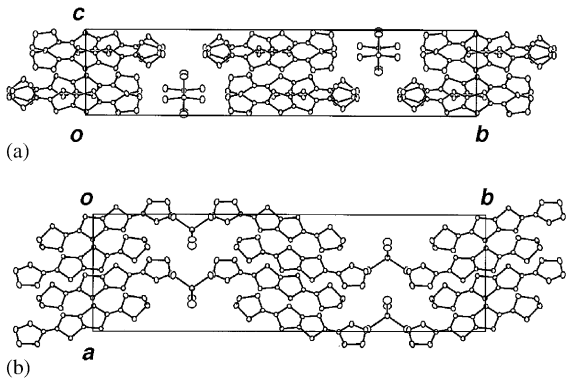

FIG. 2. Crystal structure of κ-(BDH-TTP)$_2$FeCl$_4$ viewed down the *a*-axis (a) and the *c*-axis (b). Hydrogen atoms are omitted for clarity.

The crystal structure of (BDH-TTP)$_2$FeCl$_4$ consists of κ-type sheets of BDH-TTP donor molecules and sheets of $FeCl_4^-$ anions, as illustrated in Fig. 2. The interplanar distance within a pair of donor molecules is 3.59 Å and the dihedral angle of the molecular planes between pairs is 83.3°. Compared to κ-(BDH-TTP)$_2$PF$_6$ (5), the donor packing in this salt is loose, resulting in no S···S contact shorter than the sum of the van der Waals radii (3.70 Å) within a pair of donor molecules (Fig. 3). On the other hand, there are several short S···S contacts between neighboring donor molecules located out of a pair and the large intermolecular overlap integrals are also calculated between pairs, which form two-dimensional (2D) interaction in the *ac* plane. The $FeCl_4^-$ anions are separated by the donor sheets along the *b*-axis. Within the anion sheets, consecutive anions form pairs with the Fe···Fe distance of 5.559(2) Å and the shortest Fe···Fe distance between pairs is 8.169(2) Å. So, interaction between the Fe atoms in this salt seems to be not strong.

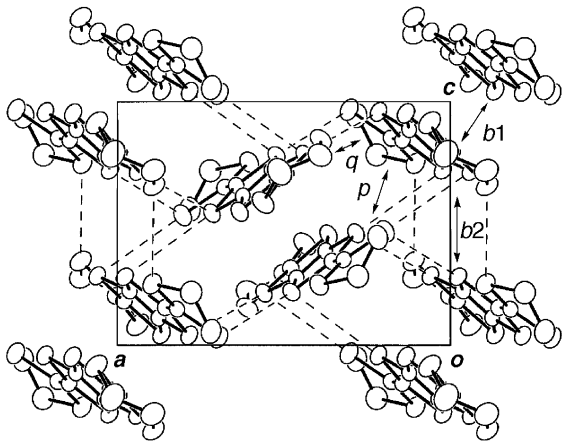

FIG. 3. Donor arrangement in κ-(BDH-TTP)$_2$FeCl$_4$ Hydrogen atoms are omitted for clarity. Intermolecular S···S contacts (<3.70 Å) are indicated by broken lines. The values of intermolecular overlap integrals ($\times 10^{-3}$) *b*1, *b*2, *p*, and *q* are 19.3, 15.7, 6.39, and −6.79, respectively.

The crystal structure of β-(BDA-TTP)$_2$FeCl$_4$ was determined both at room temperature and at 95 K. Figure 4a shows the crystal structure of this salt at room temperature, which consists of one $FeCl_4^-$ anion and two crystallographically independent BDA-TTP molecules. In this salt, the BDA-TTP molecules and the $FeCl_4^-$ anions are arranged in alternating layers along the *b*-axis, so that the Fe···Fe distance between the most adjacent anions along the *b*-axis [19.535(6) Å] is considerably longer than those along the *a*- and *c*- axes [6.227(3) and 7.731(4) Å]. At low temperature, the Fe···Fe distances along the *a*- and *c*-axes become shortened to 6.192(2) and 7.580(2) Å, respectively. Two independent BDA-TTP molecules have similar molecular structures, in both of which the two outer dithiane rings adopt non-equivalent chair conformations: their respective folding dihedral angles around the intramolecular sulfur-to-sulfur axis in one BDA-TTP molecule are 38.6° and 13.0°, and the corresponding angles in the other are 39.1° and 13.0° (Fig. 5). Thus one dithiane ring of each independent BDA-TTP molecule is much flatter than that of each BDA-TTP molecule in the superconducting BDA-TTP salts (6). Additionally, the two trimethylene end groups of each independent BDA-TTP molecule are found on the same side of the molecular plane, which is in contrast to the fact that those of the BDA-TTP molecules in both the neutral state and the superconducting slats appear with opposite orientation with respect to the molecular plane (6). The BDA-TTP molecules form slipped

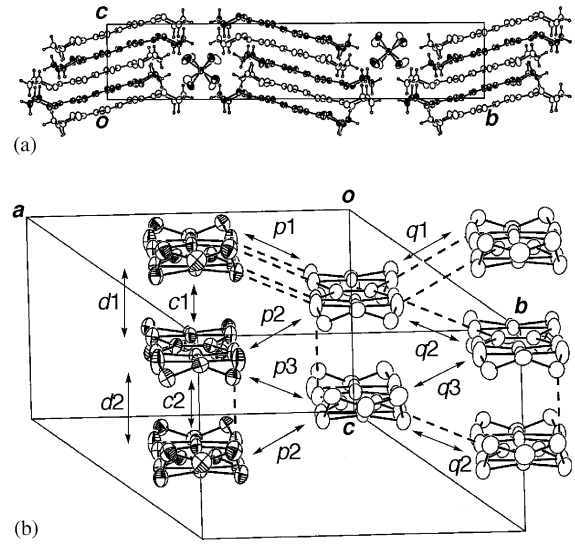

FIG. 4. (a) Crystal structure of β-(BDA-TTP)$_2$FeCl$_4$ viewed down the *a*-axis; open circles indicate the back molecules. (b) Donor arrangement of β-(BDA-TTP)$_2$FeCl$_4$. Hydrogen atoms are omitted for clarity. Interplanar distances of the BDA-TTP column are 3.56 (*d*1) and 3.89 (*d*2) Å. Intermolecular S···S contacts (<3.70 Å) are indicated by broken lines. The values of intermolecular overlap integrals ($\times 10^{-3}$) *c*1, *c*2, *p*1, *p*2, *p*3, *q*1, *q*2, and *q*3 are 14.4, 13.5, 1.88, −7.34, 3.44, 6.99, −5.62, and 5.49, respectively, whereas the corresponding values at 95 K are 15.4, 12.5, 1.49, −7.55, 3.19, 7.11, −5.65, and 5.39, respectively.

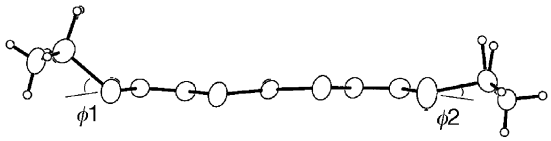

FIG. 5. Molecular structure of one BDA-TTP molecule in β-(BDA-TTP)$_2$FeCl$_4$. The dihedral angles ϕ1 and ϕ2 are 38.6° and 13.0°, whereas the corresponding angles in the other BDA-TTP are 39.1° and 13.0°. These angles at 95 K are as follows: 39.6° and 13.7°; 39.6° and 15.1°.

stacks along the *c*-axis with some dimerization (average interplanar distances of 3.56 and 3.89 Å), so as to avoid the steric hindrance of the less flat dithiane ring. There is only one S···S contact shorter than the sum of van der Waals radii within the stack, while several short intermolecular S···S contacts exist between stacks (Fig. 4b). At low temperature, although the interplanar distances in the stack are shortened to 3.47 and 3.84 Å, respectively, the number of short S···S contacts does not increase. The S···S contact pattern observed at room temperature, however, does not always reflect the magnitude of the intermolecular overlap integrals, calculated on the donor layer in the *ac* plane (10). It is noteworthy that the largest overlap integral (14.4×10^{-3}) is almost equal to those found in the superconducting BDA-TTP salts (6), suggesting that the BDA-TTP molecules in this salt are also packed loosely. This loose donor packing motif remains almost unchanged at low temperature, as can be seen from the values of the intermolecular overlap integrals shown in the caption of Fig. 4b. In addition, even at low temperature, the conformations of two independent BDA-TTP molecules are analogous to those found at room temperature.

Figure 6 shows the crystal structure of (BDA-TTP)$_3$FeCl$_4$ · PhCl, which contains layers of BDA-TTP donor molecules, alternating with layers of $FeCl_4^-$ anions. Within the anion layer, the solvent molecules (PhCl) separate the anions, and, consequently, the shortest Fe···Fe distance between adjacent anions is 8.858(1) Å, suggesting no interaction between the Fe atoms. The donor layer consists of three crystallographically independent BDA-TTP molecules (corresponding to molecules A–C shown in Fig. 6), in each of which the two outer dithiane rings prefer non-equivalent chair conformations, but, in contrast to the non-solvated β-(BDA-TTP)$_2$FeCl$_4$ salt, the two trimethylene end groups are located on both sides of the molecular plane (Fig. 7). While folding dihedral angles of the two dithiane rings in molecule C are almost equal (48.4° and 51.0°), those in the other two molecules A and B are significantly different (A, 55.8° and 35.1°; B, 28.8° and 54.0°), leading to the flat structures of molecules A and B compared to that of molecule C. Judging from the fact that the molecular structure of partially oxidized BDA-TTP molecule is flatter than that of neutral one with equivalent dithiane rings (6), molecule C would seem to be less oxidized. The difference in the degree of the charge transfer can be also appreciated by the C=C double bond lengths. The lengths of two C=C bonds [1.317(12) and 1.318(10) Å]

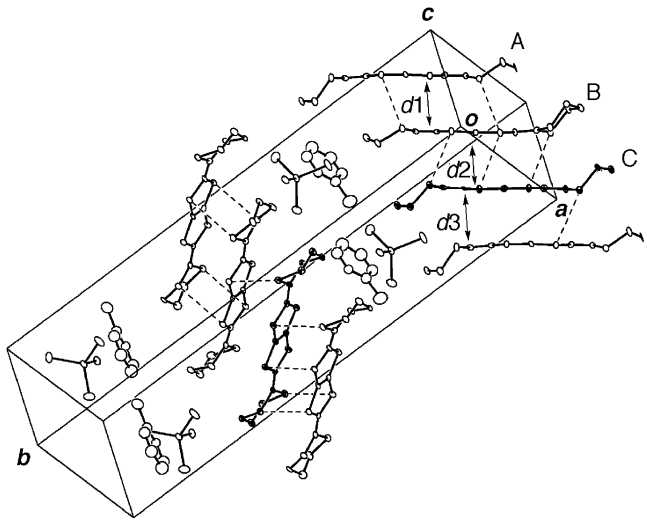

FIG. 6. (a) Crystal structure of (BDA-TTP)$_3$FeCl$_4$ · PhCl. Hydrogen atoms and some donor molecules are omitted for clarity. Molecules A and B shown by open circles correspond to the more oxidized BDA-TTP ones. Interplanar distances of the BDA-TTP column are 3.51 (*d*1), 3.62 (*d*2), and 3.66 (*d*3) Å. Intermolecular S···S contacts (<3.70 Å) are indicated by broken lines. The value of the intermolecular overlap integral between molecules A and B is -12.4×10^{-3}.

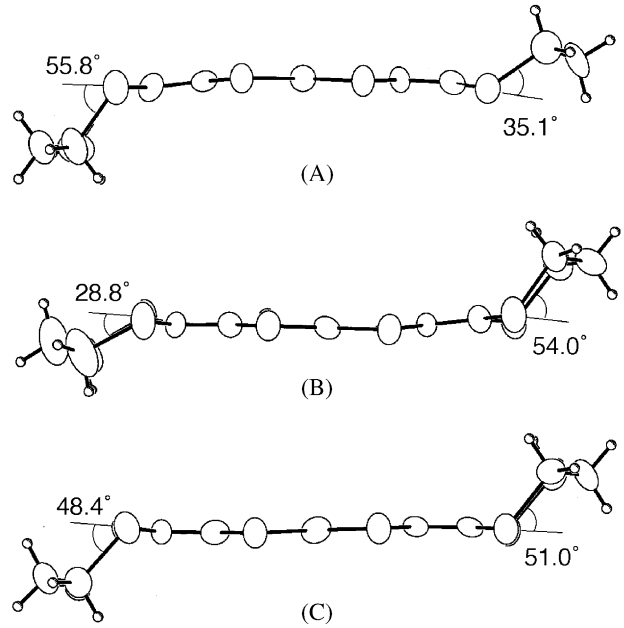

FIG. 7. Structures of three independent BDA-TTP molecules in (BDA-TTP)$_3$FeCl$_4$ · PhCl. Three C=C double bond lengths in each molecule are as follows: **A**, 1.333(13), 1.341(12), and 1.329(12) Å; **B**, 1.354(12), 1.327(12), and 1.339(12) Å; **C**, 1.317(12), 1.318(10), and 1.353(12) Å.

in molecule C are somewhat shorter than any of C=C bonds in molecules A and B, probably indicating the less oxidized state. Molecules A–C are stacked along the [10$\bar{1}$] direction with average interplanar distances of 3.51, 3.62, and 3.66 Å, and to a considerable extent mutually slipped due to the steric bulk of the dithiane ring. In the donor layer, the more oxidized molecules A and B are somewhat dimerized with the shortest interplanar distance of 3.51 Å, and no significant overlap integral is calculated between neighboring donor molecules, except for the value of the overlap integral (-12.4×10^{-3}) between the dimerized molecules A and B.

Electrical Conducting Behavior and Magnetic Properties

As expected from the crystal structure of κ-(BDH-TTP)$_2$FeCl$_4$ with 2D character similar to that found in κ-(BDH-TTP)$_2$PF$_4$, this salt exhibited a high room-temperature conductivity (σ_{rt}) of 39 S cm^{-1} and metallic conducting behavior down to 1.5 K (Fig. 8). On the other hand, the temperature dependence of its magnetic susceptibility can be well fitted to the Curie–Weiss law, and the values of the Curie and Weiss constants (C and θ) are 4.25 emu K mol^{-1} and 0.041 K, respectively. The fitted C is close to the value of 4.38 emu K mol^{-1} expected for a high-spin Fe^{+3} ion ($S = 5/2$, $g = 2.0$), so that the Fe atom in the anion certainly dominates the measured magnetization.

The resistivity of β-(BDA-TTP)$_2$FeCl$_4$ as a function of temperature indicated that this salt ($\sigma_{rt} = 9.4$ S cm^{-1}) is metallic from room temperature down to 113 K, at which temperature, it undergoes a sharp metal-to-insulator (MI) transition (Fig. 9). As a cause of this MI transition, we first anticipated the charge separation between two independent donors in the column (7). However, in this salt, no appreciable conformational change in the donor molecules occurs at 95 K, so the reason for this MI transition has not yet been elucidated. Figure 10 shows the temperature dependence of the magnetic susceptibility of this salt from 300 to 2 K. The susceptibility obeys the Curie–Weiss law ($C = 4.48$ emu K mol^{-1} and $\theta = -15.1$ K) over the whole temperature range 40–300 K. From the fitted C close to the value predicted for a high-spin Fe^{3+} ion, it can be expected that the magnetic properties of this salt are dominated by the anions. Below 40 K, the susceptibility increased to a maximum near 8.5 K, after which it decreased rapidly. As shown in the inset of Fig. 10, the susceptibilities, which were measured under the magnetic fields (1 kOe) applied along the directions approximately parallel to the crystallographic a-, b-, and c-axes, were anisotropic below near 8.5 K, indicating antiferro-

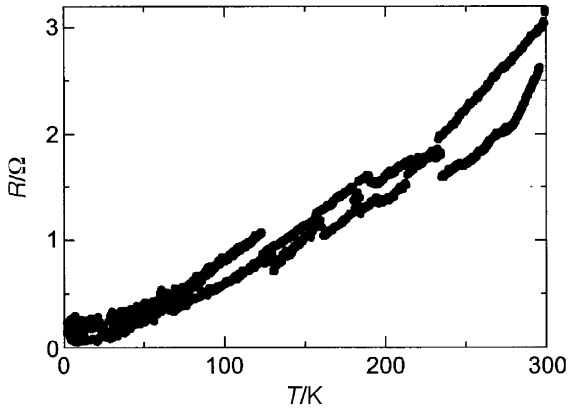

FIG. 8. Temperature dependence of the resistance of κ-(BDH-TTP)$_2$FeCl$_4$.

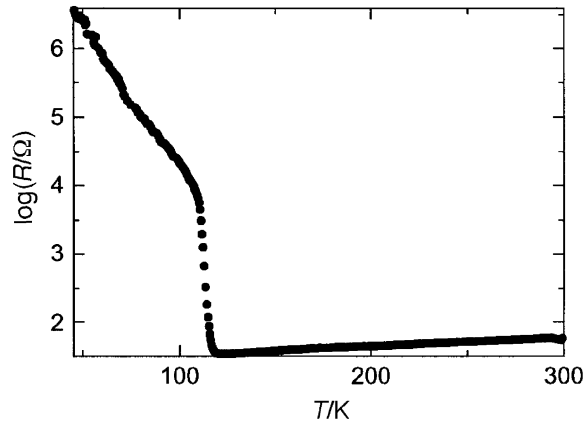

FIG. 9. Temperature dependence of the resistance of β-(BDA-TTP)$_2$FeCl$_4$.

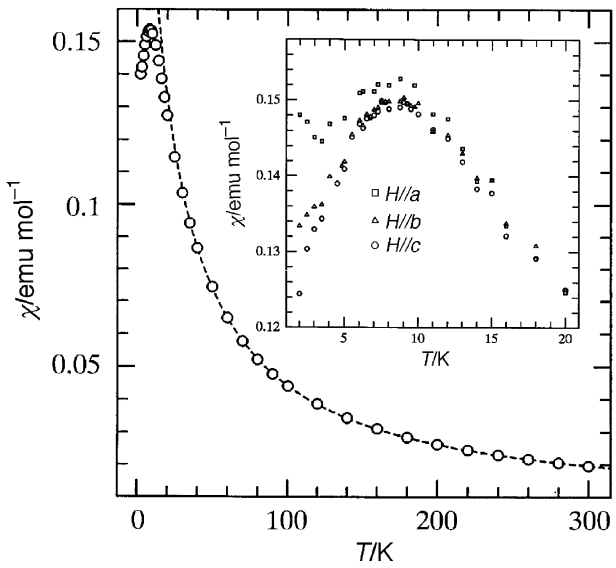

FIG. 10. Temperature dependence of the susceptibility of β-(BDA-TTP)$_2$FeCl$_4$. The dashed line is a Curie–Weiss fit (see text). The inset shows the magnetic anisotropy in magnetic fields approximately parallel to the a-, b-, and c-axes ($H \| a$, $H \| b$, and $H \| c$).

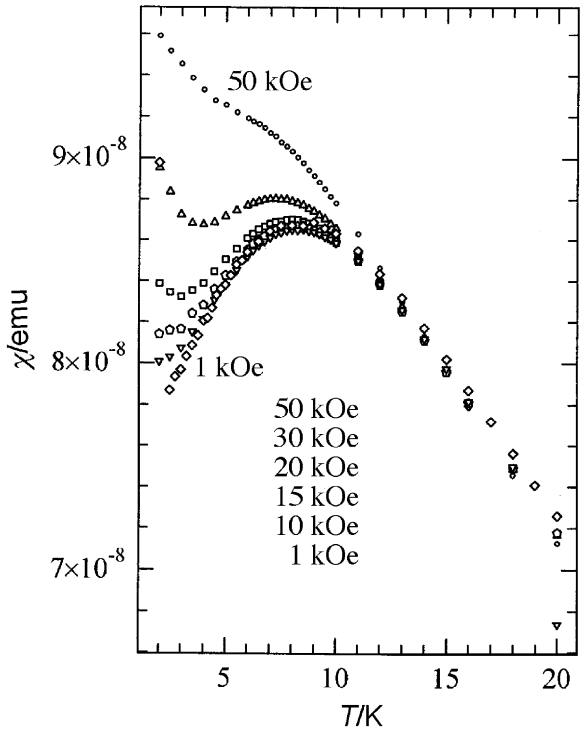

FIG. 11. Magnetic field dependence of the susceptibilities of β-(BDA-TTP)$_2$FeCl$_4$.

magnetic ordering with the Néel temperature (T_N) of near 8.5 K. Below T_N, the easy spin axis seems to lie close to the intrastacking *c*-direction of the donor molecules. So, considering that the shortest Fe···Fe distance along the *c*-axis is longer than 6 Å, the donor molecules could mediate the observed antiferromagnetic order between the Fe^{3+} ions (11). In addition, the magnetic field dependence of the susceptibilities using randomly orientated multiple crystals indicated that the antiferromagnetic transition begins to disappear near 30 kOe (Fig. 11).

Unlike metallic κ-(BDH-TTP)$_2$FeCl$_4$ and β-(BDA-TTP)$_2$FeCl$_4$ salts, the solvated (BDA-TTP)$_3$FeCl$_4$ · PhCl salt exhibited semiconducting behavior with a thermal activation energy of 0.11 eV ($\sigma_{rt} = 2.0 \times 10^{-2}$ S cm^{-1}), which is understood by considering the charge separation and weak intermolecular interaction among three independent donor molecules. In addition, this salt behaves as a Curie–Weiss paramagnet with fitted $C = 4.42$ emu K mol^{-1} and $\theta = -0.35$ K. Taking account of the fitted *C* almost equal to the value for a high-spin Fe^{+3} ion and the observed shortest Fe···Fe distance [8.858(1) Å], it is likely that the small negative Weiss constant signifies very weak antiferromagnetic interaction between the Fe moments mediated by donor molecules.

CONCLUSIONS

In order to search for non-TCF-based CT materials with multifunctional properties such as conductivity and magnetism, we focused, herein, on the preparation and study of the $FeCl_4$ salts with BDH-TTP and BDA-TTP, both of which contain the bis-fused 1,3-dithiol-2-ylidene (BDY) unit instead of the TCF unit as a π-electron system. Similar to the metallic BDH-TTP salts we so far obtained, the κ-(BDH-TTP)$_2$FeCl$_4$ salt remained metallic down to a very low temperature, but this salt did not exhibit magnetic order. On the other hand, we have succeeded in finding the first non-TCF-based salt β-(BDA-TTP)$_2$FeCl$_4$ in which metallic conductivity and antiferromagnetism can coexist. Our next target in this research area is thus the construction of a new system capable of enhancing further the interaction between conduction π-electrons of donors and localized d-spins of anions. To this end, our effort to prepare the CT salts composed of BDY donors, such as BDH-TTP and BDA-TTP, and other paramagnetic anions currently continues.

REFERENCES

1. T. Enoki, T. Umeyama, A. Miyazaki, H. Nishikawa, I. Ikemoto, and K. Kikuchi, *Phys. Rev. Let.* **81,** 3719–3722 (1998).
2. E. Coronado, J. R. Galán-Mascarós, C. J. Gómez-Garciá, and V. Laukhin, *Nature* **408,** 447–449 (2000); J. Nishijo, E. Ogura, J. Yamaura, A. Miyazaki, T. Enoki, T. Tanaka, Y. Kuwatani, and M. Iyoda, *Solid State Commun.* **116,** 661–664 (2000).
3. H. Kobayashi, A. Kobayashi, and P. Cassoux, *Chem. Soc. Rev.* **29,** 325–333 (2000); H. Fujiwara, E. Fujiwara, Y. Nakazawa, B. Z. Narymbetov, K. Kato, H. Kobayashi, A. Kobayashi, M. Tokumoto, and P. Cassoux, *J. Am. Chem. Soc.* **123,** 306–314 (2001); T. Otsuka, A. Kobayashi, Y. Miyamoto, J. Kiuchi, S. Nakamura, N. Wada, E. Fujiwara, H. Fujiwara, and H. Kobayashi, *J. Solid State Chem.* **159,** 407–412 (2001), doi:10.1006/jssc.2001.9172.
4. M. Iwamatsu, T. Kominami, K. Ueda, T. Sugimoto, T. Adachi, H. Fujita, H. Yoshino, Y. Mizuno, K. Murata, and M. Shiro, *Inorg. Chem.* **39,** 3810–3815 (2000).
5. J. Yamada, M. Watanabe, H. Anzai, H. Nishikawa, I. Ikemoto, and K. Kikuchi, *Angew. Chem. Int. Ed.* **38,** 810–813 (1999).
6. J. Yamada, M. Watanabe, H. Akutsu, S. Nakatsuji, H. Nishikawa, I. Ikemoto, and K. Kikuchi, *J. Am. Chem. Soc.* **123,** 4174–4180 (2001).
7. For a preliminary communication on β-(BDA-TTP)$_2$FeCl$_4$ and (BDA-TTP)$_3$FeCl$_4$ · PhCl, see: J. Yamada, T. Toita, H. Akutsu, S. Nakatsuji, H. Nishikawa, I. Ikemoto, and K. Kikuchi, *Chem. Commun.* 2538–2539 (2001).
8. H. Anzai, J. M. Delrieu, S. Takasaki, S. Nakatsuji, and J. Yamada, *J. Cryst. Growth* **154,** 145–150 (1995); H. Nishikawa, T. Sato, T. Kodama, I. Ikemoto, K. Kikuchi, H. Anzai, and J. Yamada, *J. Mater. Chem.* **9,** 693–696 (1999).
9. T. Mori, A. Kobayashi, Y. Sasaki, H. Kobayashi, G. Saito, and H. Inokuchi, *Bull. Chem. Soc. Jpn.* **57,** 627–633 (1984).
10. T. Mori, *Bull. Chem. Soc. Jpn.* **71,** 2509–2526 (1998).
11. H. Tanaka, T. Adachi, E. Ojima, H. Fujiwara, K. Kato, H. Kobayashi, A. Kobayashi, and P. Cassoux, *J. Am. Chem. Soc.* **121,** 11243–11244 (1999).